Density of states of helium droplets

Klavs Hansen[*]

Department of Physics, Göteborg University, SE-412 96 Göteborg, Sweden

Michael D. Johnson and Vitaly V. Kresin

Department of Physics and Astronomy, University of Southern California, Los Angeles, California 90089-0484, USA

(Received 10 September 2007; published 21 December 2007)

Accurate analytical expressions for the state densities of liquid ^{4}He droplets are derived, incorporating the ripplon and phonon degrees of freedom. The microcanonical temperature and the ripplon angular momentum level density are also evaluated. The approach is based on inversions and systematic expansions of canonical thermodynamic properties.

PACS number(s): 67.40.Db, 67.40.Kh

I. INTRODUCTION

Important dynamical processes in finite systems such as nuclei, polyatomic molecules, nanoclusters, atomic clouds, and droplets frequently turn out to be statistical in nature: evaporation/fragmentation, radiation, emission of electrons, and equilibration between internal degrees of freedom or between host and solvent molecules. When such a system is thermally isolated, e.g., when flying in a beam or suspended in a trap, the proper statistical-mechanics treatment is that of the microcanonical ensemble where the energy E is fixed and not the temperature of an external heat bath. The density of states, or level density, $\rho(E)dE$ represents the number of quantum states between energy E and $E+dE$. For separable degrees of freedom, this is the number of normal mode combinations such that their energies add up to a total internal energy lying in this interval. This function plays a crucial role in the thermal description of microcanonical systems. For low excitation energies, $\rho(E)$ can be represented by a sum of delta functions, corresponding to excitations of only a few of the individual modes, but for even moderate excitation energies, the density of these delta functions becomes so large that it is well described as a continuous function of energy. In this situation, it is most convenient to use a density smoothed over the discreteness of the energy levels. In addition to energy, systems described with the microcanonical ensemble have a conserved total angular momentum, so the correspondingly resolved density of states, $\rho(E,J)$, is often of relevance.

Free liquid helium nanodroplets[1,2] represent an interesting system for a statistical treatment. One reason is that helium is the only element which cannot be described in terms of classical dynamics for any internal degrees of freedom under the experimental conditions used to study the droplets. This makes the system interesting in its own right. For example, "magic number" maxima in the size distributions of small ^{4}He clusters have been shown to correlate with the ability of the cluster to accommodate elementary excitation modes.[3] A second reason is the use of the droplets as microcryostats used to investigate other clusters and molecules. Evaporative cooling generates internal energies corresponding to temperatures of ≈ 0.4 K and is used to thermalize impurities to this otherwise unreachable temperature for gas phase mol-

ecule and cluster beams. Understanding these processes requires accurate density-of-states expressions for the elementary excitation spectrum.

The calculation of level densities requires that the excitation spectrum is known. At low temperatures, the relevant normal modes of ^{4}He$_N$ clusters within the liquid drop model are ripplons which are quantized capillary surface waves, and phonons which are quantized bulk compression waves.[4] For large droplets, these modes are separable to a good approximation,[5] a fact that greatly facilitates a statistical analysis of the excitation spectrum. For a spherical droplet, both ripplon and phonon modes possess well-defined eigenvalue spectra characterized by angular momentum for ripplons, and angular momentum and mode index for phonons. A calculation of the total density of states requires enumeration of all possible normal mode combinations, with individual energies and angular momenta adding up to a given total E and J.

A leading-order evaluation of $\rho(E)$ for ripplons was carried out by Brink and Stringari.[6] Subsequently, Lehmann[7] presented a comprehensive discussion of the densities of states for ripplons and phonons computed by direct numerical counting, and showed that the resultant plots of the logarithm of the level densities could be well parametrized by polynomial fits. These fits were then used to calculate other thermodynamic functions and to analyze droplet cooling with angular momentum conservation constraints.[8,9]

In this paper, we show that accurate density of states functions can be obtained by analytic evaluation. This is appealing in its own right, as the calculations take advantage of several elegant and generally useful tools from the literature. In addition, having analytic expressions for various types of elementary excitations provides a systematic method for treating situations where several types of normal modes are excited simultaneously, or when the spectrum of elementary excitations is modified.

The plan of the paper is as follows. In Sec. II, we calculate the ripplon density of states as a function of energy, Sec. III considers its angular momentum dependence, Sec. IV is devoted to phonon excitations, Sec. V to the angular momentum of phonons, and Sec. VI to the total $\rho(E)$ function. Section VII comments on the similarity between the spectra considered here and those of multielectron bubbles in bulk liquid helium, and presents a summary.

II. RIPPLON DENSITY OF STATES

As mentioned above, ripplons are quantized waves on the droplet surface. For a spherical liquid drop, the elementary excitation spectrum is given by[10]

$$\varepsilon_\ell = \hbar\omega_0 \sqrt{\ell(\ell-1)(\ell+2)}. \tag{1}$$

Here, $\ell \geq 2$ is the angular momentum quantum number of the wave and

$$\omega_0 = \sqrt{\frac{\sigma_t}{DR^3}} = \sqrt{\frac{4\pi\sigma_t}{3m_a N}}, \tag{2}$$

where σ_t is the coefficient of surface tension, D the mass density, R the droplet radius, m_a the atomic mass, and N the number of atoms in the droplet. If the parameters of bulk liquid helium are used, we have $\hbar\omega_0 \approx (3.8/\sqrt{N})$K in temperature units.[7] Below, the ripplon energy will be expressed in dimensionless units scaled to the quantity $\hbar\omega_0$. Each mode has a degeneracy of $(2\ell+1)$.

A. Canonical approximation

A first approximation to the level density can be derived in the canonical ensemble picture, where it is assumed that the system possesses a definite temperature T, and the system's internal energy is associated with its most probable value. The energy density of states of a finite system is then given by[6,11–13]

$$\rho(E) = \frac{e^S}{\sqrt{-2\pi(\partial E/\partial\beta)}}, \tag{3}$$

where $\beta \equiv (k_B T)^{-1}$ and

$$S = \beta E + \ln Z \tag{4}$$

is the entropy; Z is the canonical partition function. In the following, we will use units where $k_B=1$. The square root appearing in the equation involves the heat capacity and appears because the canonical entropy includes an approximately Gaussian integral over the thermally populated states with a width given by the heat capacity and the temperature, see, e.g., Ref. 13.

Since the ripplon elementary excitations are bosons, we have

$$\ln Z = - \sum_{\ell=2}^{\ell_{max}} (2\ell+1)\ln(1 - e^{-\beta\varepsilon_\ell}). \tag{5}$$

The canonical thermal energy of the ripplon ensemble is

$$E = - \partial(\ln Z)/\partial\beta. \tag{6}$$

To leading order, we can replace the sum in Eq. (5) by an integral from zero to infinity, and approximate the energy eigenvalues [Eq. (1)] by $\varepsilon_\ell \approx \ell^{3/2}$. The integral then straightforwardly evaluates to

$$\ln Z = \Gamma\left(\frac{7}{3}\right)\zeta\left(\frac{7}{3}\right)\beta^{-4/3} = 1.685\beta^{-4/3}, \tag{7}$$

and from Eq. (6), the (dimensionless) energy is

$$E = 2.247\beta^{-7/3}. \tag{8}$$

Assembling everything into Eq. (3) and expressing the answer in terms of the energy, we find

$$\rho_{rip}(E) \approx 0.311 E^{-5/7} \exp(2.476 E^{4/7}), \tag{9}$$

which is the same answer as in Ref. 6.

B. Microcanonical ensemble

The above calculation can be improved in two places. One obvious refinement is to evaluate the sum [Eq. (5)] with greater care and to use more precise eigenvalues. A deeper conceptual question is how to compute thermodynamic quantities for a finite isolated system for which the total internal energy is a conserved quantity and not an expectation value and the use of "temperature" must be carefully defined. A thorough discussion was given by Andersen *et al.* in Ref. 13 with the conclusion that the convenient canonical formalism may be retained, but the canonical expression for the energy [Eq. (6)] must be corrected as follows:

$$E = - \partial(\ln Z)/\partial\beta - \beta^{-1}. \tag{10}$$

Here, E is the fixed excitation energy of the system and β is understood as the "microcanonical temperature" defined as

$$\beta \equiv \partial[\ln \rho(E)]/\partial E. \tag{11}$$

The procedure taken is as follows. First, the sum in Eq. (5) is calculated using the first three terms of the Euler-Maclaurin summation formula.[14] With the form of the spectrum given in Eq. (1), this formula becomes

$$-\ln Z = \int_2^\infty (2\ell+1)\ln(1 - e^{-\beta\varepsilon_\ell})d\ell + \frac{5}{2}\ln(1 - e^{-\beta\varepsilon_2})$$

$$- \frac{1}{12}\frac{d}{d\ell}[(2\ell+1)\ln(1 - e^{-\beta\varepsilon_\ell})]\Big|_{\ell=2} + \cdots. \tag{12}$$

The upper limit, ℓ_{max}, has been set to infinity as before. The actual value is on the order of $\ell_{max} \approx 2\pi R/\lambda_{min} \approx 2\pi R/(2d)$, where λ is the wavelength and d is the interatomic distance.[5] In the liquid drop approximation $(R=N^{1/3}d/2)$, one then has $\ell_{max} \approx \pi N^{1/3}/2$. In view of Eqs. (1) and (2), this yields a size-independent ripplon Debye temperature of $\varepsilon_{max} \approx 7.5$ K. Using this value to estimate the error in $\ln Z$, the leftover terms are found to be on the order of $(\beta\varepsilon_{max}/4 - 7\ell_{max}/6)\exp(-\beta\varepsilon_{max})$. For $T=1$ K, this is a relative contribution to $\ln Z$ of less than $10^{-2}/N^{1/3}$ which will be ignored.

A tedious calculation of Eq. (12) involving expansions of exponentials in powers of β is given in the Appendix. The result is

$$\ln Z = 1.685\beta^{-4/3} + 0.639\beta^{-2/3} - \frac{349}{96} + \frac{7}{3}\ln(2\sqrt{2}\beta) + \cdots. \tag{13}$$

The first term coincides with Eq. (7), and the rest are finite-size and spectral corrections. Note that all the numerical coefficients derive from explicit expressions involving special functions. The expansion Eq. (13) has been checked against
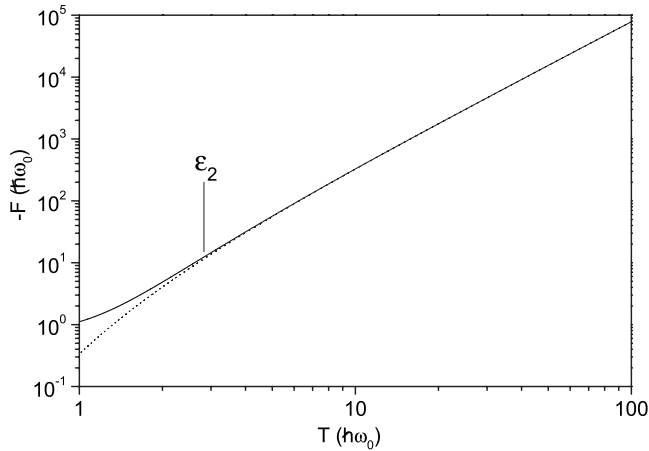
FIG. 1. The (negative of) the ripplon free energies, calculated with Eq. (13) (dotted line) and the summation in Eq. (5) (full line) which is exact apart from setting the upper limit to infinity. The temperature corresponding to the energy of the lowest excitation ε_2 is indicated.

a numerical sum. The comparison is shown in Fig. 1 for Helmholtz free energy, $F = -T \ln Z$. Already at temperatures where T is equal to the lowest excitation energy $\varepsilon_2 = \hbar \omega_0 \sqrt{6}$ is the free energy well represented by the above expression. At higher energies, the agreement improves monotonically.

Knowing the partition function, we can now use Eq. (10) to determine the relation between the microcanonical energy and temperature,

$$E = 2.247 \beta^{-7/3} + 0.426 \beta^{-5/3} - \frac{10}{3} \beta^{-1}. \quad (14)$$

Again, the first term reproduces Eq. (8).

In order to proceed with the calculation of the entropy, the heat capacity and the level density in Eq. (3), we need to invert relation (14) which expresses $E(\beta)$ to get $\beta(E)$. This is done by the iterative method of successive approximations, as outlined in the Appendix. The result is an expansion for β^{-1} in powers of $E^{-2/7}$,

$$\beta^{-1} = 0.7069 E^{3/7} - 0.072\,39 E^{1/7} + 0.7212 E^{-1/7} + \cdots, \quad (15)$$

where the coefficients are calculated from those entering Eq. (14). Now, the prefactor and the exponent in Eq. (3) can be evaluated using Eqs. (4), (13), and (14) and $\beta(E)$, finally yielding

$$\rho_{rip}(E) = 0.205 E^{-12/7} \exp(2.476 E^{4/7} + 0.507 E^{2/7}). \quad (16)$$

Let us emphasize again that all the numerical coefficients encode analytical expressions.

Equation (16), which is the main result of this section, may be compared with the canonical approximation [Eq. (9)], an exact numerical count carried out with the help of the Beyer-Swinehart algorithm,[15] and the form written down in Ref. 7 as an empirical fit to the numerical count in the interval $E = 50-2500$. Figure 2 shows such a comparison and
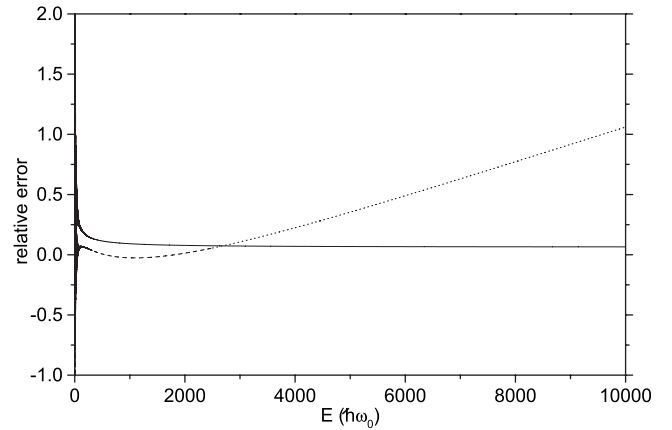

FIG. 2. Comparison of the ripplon level densities calculated according to Eq. (16) (full line) and Ref. 7 (dashed for $E < 2500$ and dotted line for $E > 2500$). The fit in Ref. 7 was limited to energies between 50 and 2500 in the reduced units used here and is calculated as the derivative of the numerical fit to the integrated level density. The expressions have been divided by the exact Beyer-Swinehart result, causing the oscillatory behavior at low energy, and the curves plotted are the logarithms of these ratios. The curve of Ref. 6 (not shown) is around 3.

demonstrates that the analytical expression gives an excellent representation of the exact result.[16]

III. RIPPLON ANGULAR MOMENTUM DENSITY

The next step is to generalize the ripplon state density to a function which is not only energy but also angular momentum resolved. This problem has been comprehensively studied in nuclear physics.[11,12] One way of visualizing the net angular momentum of a large distribution of excitations with varying (ℓ, ℓ_z) is as the result of random angular momentum coupling, in which case the central limit theorem applies and one expects to find a normal distribution. Indeed, the above references show that $\rho(E, J)$ is essentially a product of $\rho(E)$ and a Gaussian factor,

$$\rho(E, J) = \rho(E) \frac{2J + 1}{2(2\pi)^{1/2} \sigma^3} e^{-J(J+1)/2\sigma^2}. \quad (17)$$

It is permissible here to replace $J(J+1)$ by $(J + \frac{1}{2})^2$.

It is still necessary to establish the variance σ^2. An elegant way to do this to leading order by means of an extended grand canonical distribution is described in Bethe's review,[11] where the method is applied to a system of noninteracting fermions in a spherical potential box. Here, we follow the same procedure for a system of bosonic ripplon excitations.

The idea is to first evaluate the projection M of the net angular momentum $\vec{J}$ of the droplet in terms of the contributions of individual normal modes at temperature T. The fact that M is a conserved quantity is accounted for by a separate Lagrange multiplier or a "chemical potential" γ, such that

$$\gamma = -\partial S / \partial M \quad (18)$$

(S is the entropy). We can calculate M directly by summing over all modes,

$$M = \sum_{\ell=2}^{\infty} \sum_{m=-\ell}^{\ell} \frac{m}{e^{\beta \varepsilon_\ell - \gamma m} - 1} \approx \int_0^{\infty} d\ell \int_{-\ell}^{\ell} \frac{m \, dm}{e^{\beta \ell^{3/2} - \gamma m} - 1}$$
(19)

(in reduced energy units). Expanding the integrand to first order in γ,[11] we find

$$M = \frac{20}{27} \Gamma\left(\frac{5}{3}\right) \zeta\left(\frac{5}{3}\right) \gamma \beta^{-4/3},$$
(20)

and Eq. (8) allows us to express the result in terms of the droplet energy. To leading order, we have

$$\gamma = 1.776 M E^{-8/7}.$$
(21)

Now, we can use Eq. (18) with Eq. (21) to obtain the entropy variation,

$$S(E, M) = S(E, 0) - M^2/(2\sigma^2),$$
(22)

with

$$(2\sigma^2)^{-1} = 0.888 E^{-8/7}.$$
(23)

The second term in Eq. (22) leads to a normal distribution in M. The distribution in J can be shown to have the same variance.[11,12] Therefore, Eqs. (17) and (23) define $\rho_{rip}(E, J)$.

The numerical evaluation of the rotational density of states in Ref. 7 led to essentially the same form of the state density function, with the factor corresponding to $(2\sigma^2)^{-1}$ fitted as $0.868 E^{-8/7} + 0.964 E^{-13/7}$, which affirms the analytical result [Eq. (23)]: the factors deviate by less than 2% for $E = 100$–2500.

A shorter estimate of the variance is illustrative. The number of quanta in one mode (ℓ, m) is on the order of T/ε_ℓ for levels up to $\varepsilon_\ell \simeq T$ and zero for higher quantum energies. The total number of excited quanta is then

$$n \approx \sum_{\ell=2}^{T^{2/3}} (2\ell + 1) T/\ell^{3/2} \approx 4 T^{4/3},$$
(24)

where the sum was approximated by an integral and T is written in terms of the ω_0 unit. With the energy-temperature relation [Eq. (14)], we get the leading order value for energy per quantum $\langle e \rangle = E/n = 2.247 T/4$, and from this, an average of $\langle \ell \rangle = \langle e \rangle^{2/3} = T^{2/3}(2.247/4)^{2/3}$. The standard deviation σ of ℓ is then, according to the "random walk" argument used above, $\sigma = \sqrt{n} \langle \ell \rangle$. Inserting the calculated $\langle \ell \rangle$ and expressing the result in terms of the total energy, one has

$$(2\sigma^2)^{-1} = 2^{-1/3}(2.247)^{-4/21} E^{-8/7} = 0.68 E^{-8/7},$$
(25)

in surprisingly sensible agreement with the above result.

One may seek to describe the angular momentum distribution in the language of a rotational energy and a moment of inertia I, associating[12] the exponential in Eq. (17) with a Boltzmann factor involving $\beta \hbar^2 J(J+1)/(2I)$, i.e., $I = \hbar^2 \beta \sigma^2$. Using the canonical-ensemble results [Eqs. (8) and (23)], we can express the "ripplon moment of inertia" in terms of the ripplon excitation energy (in reduced units),

$$I = 0.797 E^{5/7}.$$
(26)

IV. PHONON DENSITY OF STATES

Surface ripplons are the lowest-temperature droplet excitations; bulk phonons appear next. These are compression sound waves which arise as solutions of the wave equation within the volume of the spherical drop. As such, their energies are given by

$$\varepsilon_{n,\ell} = \hbar u k_{n,\ell},$$
(27)

where u is the speed of sound and the wave number $k_{n,\ell}$ is determined by the boundary condition at the surface. If the Dirichlet boundary condition is adopted,[5,7] then $k_{n,\ell} = a_{n,\ell}/R$, where $a_{n,\ell}$ is the nth root of the j_ℓ spherical Bessel function. For a free surface, a more appropriate boundary condition is the Neumann one, in which case $k_{n,\ell} = a'_{n,\ell}/R$, with $a'_{n,\ell}$ the root of the Bessel function derivative j'_ℓ. The energy scale is set by the longest wave length, i.e., $k \sim \pi/R$, so we can express phonon energies in units of

$$\tilde{\varepsilon} = \hbar u \pi/R,$$
(28)

which works out to $\tilde{\varepsilon} = (25.5 N^{-1/3}) K$ in temperature units if the speed of sound in bulk ^{4}He is used.[7] The leading-order behavior of the phonon state density can be determined in a straightforward way by invoking the standard expression for the Debye heat capacity (per unit volume) of bulk phonons,[17]

$$C_{bulk} = \frac{2\pi^2}{15} \frac{k_B^4}{\hbar^3 u^3} T^3.$$
(29)

Multiplying this by $4\pi R^3/3$ and using the fact that (in the canonical framework) $C = \partial E/\partial T$ and $(k_B T)^{-1} = \partial S/\partial E$, we can use integrations to express S in terms of E. Then, from Eq. (3), we find that to first order, $\ln \rho_{ph}(E) \approx S(E) = 3.41 E^{3/4}$. This matches the leading term of the fit to a direct numerical count in Ref. 7 which is $3.331 E^{3/4}$.

The Debye temperature for phonons in liquid ^{4}He is ≈ 25 K,[22] corresponding to a total phonon thermal energy [from Eq. (31)] of $\approx 1000 N$ K. We can therefore use the low temperature approximation throughout.

The prospect of refining the calculation by analytically evaluating a statistical sum over the precise spectrum [Eq. (27)] may seem bleak, as the Bessel function roots which "contribute in an essential manner are just the zeros for which the usual formulas (such as McMahon's expansion) are bad approximations."[18] However, rescue comes from an elegant mathematical framework known as the Weyl expansion.[18–20] It provides a systematic expression for the smoothed density of eigenmodes in a finite cavity in terms of volume, surface, and curvature terms. As described in the above references, this is a very general theory, valid for both scalar and vector wave equations, and applicable to a wide variety of physical phenomena.

Reference 21 applied this formalism to the specific heat of metal nanoparticles. The finite-size correction to the specific heat [Eq. (29)] derived there is immediately usable for our droplet problem,

$$C = C_{bulk} \pm \frac{9\zeta(3)}{4\pi} \frac{k_B^3}{\hbar^2 u^2} \frac{T^2}{R} + \frac{1}{6} \frac{k_B^2}{\hbar u} \frac{T}{R^2}. \qquad (30)$$

The $+$ sign applies to the Neumann and the $-$ sign to the Dirichlet boundary conditions. Although we focus on the Neumann condition, the Dirichlet case will be included for completeness.

We now follow almost the same sequence as in the bulk limit described above: Eq. (30) is multiplied by the droplet volume and integrated once to obtain (with E and T in units of $\tilde{\varepsilon}$)

$$E(T) = \frac{2\pi^6}{45} T^4 \pm \zeta(3)\pi^2 T^3 + \frac{\pi^2}{9} T^2, \qquad (31)$$

and a second time to obtain $S(T)$ as $S = \int_0^T (C/T')dT'$. The first function is inverted by iteration to yield

$$T(E) = 0.391E^{1/4} \mp 0.069 - 0.006E^{-1/4}. \qquad (32)$$

[Calculating $T(E)$ instead of $\beta(E)$ is more convenient in this case.] Equation (3) is then used to obtain the density of states. The calculation is done to the first three orders in E, in correspondence to the three terms in the heat capacity expansion [Eq. (30)]. The microcanonical correction [Eq. (10)] in the present case turns out to contribute only in the next order of smallness. The result of the calculation is as follows:

$$\rho_{ph}(E) = AE^{-5/8} \exp(3.409E^{3/4} \pm 0.908E^{1/2} + 0.482E^{1/4}). \qquad (33)$$

Once again, the $+$ sign is for the Neumann boundary condition on the phonon wave at the droplet surface and the $-$ for the Dirichlet condition. Using the bulk canonical heat capacity in Eq. (30) gives a preexponential factor of $A = 0.26$.

Figure 3 compares the exact Beyer-Swinehart count for the phonon spectrum with the full Eq. (33) and with the level density based on the bulk Debye heat capacity [Eq. (29)], i.e., where only the first term in the exponent is present. Figure 4 shows a more detailed comparison of Eq. (33) and the exact-count phonon level density. We find good agreement between the analytical expression and the exact computation, although not as good as for the ripplon case.

The estimate of the prefactor A in Eq. (33) cannot be expected to be correct because it does not include higher-order expansion terms in the exponent that would yield corrections of the same order. A comparison with the numerical count suggests a correction in the form of a factor $\exp(-0.62E^{0.2})$. Although this correction is larger than the error found for the ripplon level density, it is nevertheless still relatively small. An effective value of $A \approx 0.05$ can be used for energies below 400.

V. PHONON ANGULAR MOMENTUM DENSITY

A computation of the angular momentum resolved phonon level density suffers from the difficulties with expressing the lowest Bessel function eigenvalues with a simple functional form. In contrast to $\rho_{ph}(E)$ there is, to our knowledge, no solution in the literature for this problem. As will be clear from the results presented in Sec. VI below, the contribution
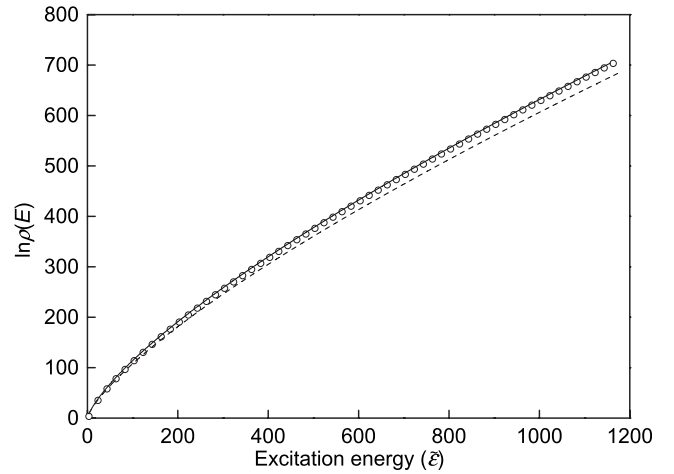

FIG. 3. Phonon level densities calculated according to the exact Beyer-Swinehart count (open circles), Eq. (33) (full line), and the level density derived from the bulk Debye heat capacity, i.e., corresponding to Eq. (33) but including only the first term in the exponential (dashed line).

to the level density from the phonons is minor compared to that of the ripplons, and the required precision in the calculation of the angular specified phonon contribution is therefore correspondingly smaller. In this section, we will make an order of magnitude estimate, based on the leading order term of McMahon's expansion of the roots of the Bessel functions.[14] For the Neumann boundary condition, the roots are $(n+\ell/2-3/4)\pi \approx (n+\ell/2)\pi$. With the phonon energy scale used [Eq. (28)], the quantum energies are thus $n+\ell/2$. When states with energies up to T are averaged, the linear dependence of the quantum energy on ℓ gives an average value of $\langle \ell \rangle \sim T$. Since the n dependence also is linear, the constant of proportionality is on the order of unity. The total number of states below energy T is on the order of T^3. Combining these estimates gives, using the same type of random walk estimate as Eq. (25) for the ripplons, that
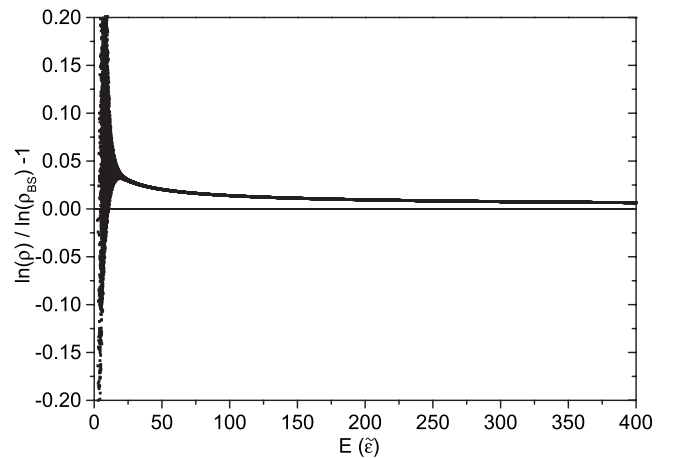

FIG. 4. A comparison of Eq. (33) and the exact-count phonon level density, showing essentially the relative difference in the entropy of the phonon system in the two calculations.

$$(2\sigma_{ph}^2)^{-1} \sim \frac{1}{T^3 T^2} = \left(\frac{2\pi^6}{45}\right)^{5/4} E^{-5/4} \approx 100 E^{-5/4}. \quad (34)$$

The ratio of the σ's for the phonons and ripplons (here denoted σ_{rip}) with the leading order terms in the caloric curves Eqs. (14) and (31) and the proper energy scaling is

$$\frac{\sigma_{ph}}{\sigma_{rip}} \sim 0.002[T \text{ (K)}]^{7/6} N^{1/6}. \quad (35)$$

This is small compared to unity up to extremely large droplet sizes. The conclusion that the width of the phonon angular momentum distribution can be ignored holds very well, even if the estimate of the width were incorrect by as much as an order of magnitude.

VI. COMBINED LEVEL DENSITY

A helium droplet may have both ripplon and phonon oscillations excited at the same time (and, at higher temperatures, rotons as well[1]). The coupling between these normal modes is weak at bulk liquid surfaces[23] and in large droplets;[5] thus, their energy contents may remain independently defined for some length of time, and the individual state densities will then come from Eqs. (16) and (33). The question of equilibration dynamics of excitations in superfluid droplets and the relevant time scales is a very interesting one, and has not yet been addressed in detail. Below, we discuss an estimate of state densities in circumstances when the ripplon and phonon excitations do achieve statistical equilibrium.

In principle, the level density of combined excitations can be calculated by the method used in Sec. II for the ripplon degrees of freedom alone. This would be a very involved procedure because the ripplon and phonon quantum energies have different dispersion relations and scale differently with size. Alternatively, one can calculate the level density as a convolution. In this task, one also benefits from formulating the general problem in terms of the microcanonical temperature. The convolution to be performed is

$$\rho(E) = \int_0^E \rho_{rip}(E - \varepsilon) \rho_{ph}(\varepsilon) d\varepsilon. \quad (36)$$

For not extremely large droplets, the largest part of the excitation energy resides in the ripplons. Indeed, the ratio between the energies of the ripplon and phonon subsystems is canonically,

$$\frac{E_{ph}}{E_{rip}} \approx 6.8 \times 10^{-3} N^{1/3} [T \text{ (K)}]^{5/3} \quad (37)$$

(temperature expressed in kelvins). It is clear that for temperatures under 1 K (i.e., those which lie safely below the Debye cutoff values specified above and below the onset of roton modes) and droplets of up to several tens of thousands of atoms in size, the phonon energy contents is a fraction of the ripplon energy. Under these conditions, one can treat the ripplon degrees of freedom as a heat bath and calculate the phonon contribution with an expansion of the integrand of

Eq. (36) around some small phonon energy. We will use the simplest choice of zero phonon energy, and to increase the precision, we expand the *logarithm* of the level density. Thus,

$$\rho(E) = \int_0^E \rho_{rip}(E) \exp\left[-\varepsilon \frac{d \ln[\rho_{rip}(E)]}{dE} \right.$$
$$\left. + \frac{1}{2}\varepsilon^2 \frac{d^2 \ln[\rho_{rip}(E)]}{dE^2} - \cdots \right] \rho_{ph}(\varepsilon) d\varepsilon. \quad (38)$$

The upper limit of the integral can be replaced by infinity without serious loss of precision because the integrand peaks well below this value. We recognize the first derivative in the exponential as the microcanonical temperature $1/T$ of the ripplon system at energy E [see Eq. (11)], and therefore have

$$\rho(E) = \rho_{rip}(E) \int_0^\infty e^{-\varepsilon/T} \rho_{ph}(\varepsilon)$$
$$\times \exp\left[\frac{1}{2}\varepsilon^2 \frac{d^2 \ln[\rho_{rip}(E)]}{dE^2} + \cdots \right] d\varepsilon. \quad (39)$$

The second exponential in the integrand can be expanded, with the integral of the first term yielding the phonon canonical partition function at T, $Z_{ph}(T)$,

$$\rho(E) = \rho_{rip}(E) \left\{ Z_{ph}(T) + \int_0^\infty e^{-\varepsilon/T} \rho_{ph}(\varepsilon) \right.$$
$$\left. \times \left[\frac{1}{2}\varepsilon^2 \frac{d^2 \ln[\rho_{rip}(E)]}{dE^2} + \cdots \right] d\varepsilon \right\}. \quad (40)$$

To leading order and ignoring the difference between the canonical and microcanonical temperatures, this simplifies to

$$\rho(E) = \rho_{rip}(E) Z_{ph}(T) \left\{ 1 - \frac{C_{ph}}{2C_{rip}} - \frac{E_{ph}^2}{2C_{rip}T^2} + \cdots \right\}. \quad (41)$$

Hence, the ratio of the term which is second order in ε to the zero order term in Eq. (40) is approximately

$$\frac{C_{ph}}{2C_{rip}} + \frac{E_{ph}^2}{2C_{rip}T^2} = 6 \times 10^{-3} [T \text{ (K)}]^{5/3} N^{1/3}$$
$$+ 4 \times 10^{-6} [T \text{ (K)}]^{14/3} N^{4/3}. \quad (42)$$

For not excessively large or warm droplets, we can leave out the correction terms and thus have

$$\rho(E) = \rho_{rip}(E) Z_{ph}(T), \quad (43)$$

where $Z_{ph}(T)$ as stated above is the phonon canonical partition function at the microcanonical ripplon temperature corresponding to the ripplon energy E.

The exponential part of the phonon canonical partition function can be calculated, e.g., by integration of the standard relation Eq. (6) with the caloric curve in Eq. (31). This procedure does not determine the integration constant which translates into a multiplicative constant on the total level density [Eq. (43)]. This constant c is approximately the product of the preexponential from Eq. (33) and the prefactor that appears in Eq. (3) (i.e., the value given by a saddle point
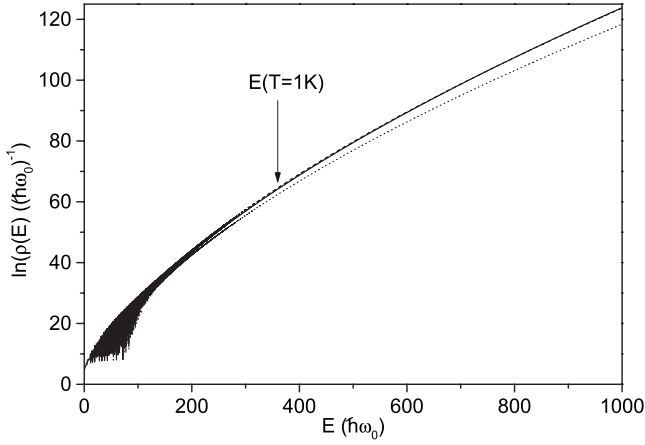
FIG. 5. The convoluted level densities for phonons and ripplons for droplet size 10^3. The numerical convolution is the full line, and the approximate result in Eq. (45) is the (hardly discernible) dashed line. The level densities for ripplons alone (dotted line) is given for reference. The arrow indicates the energy content of the combined ripplon-phonon system in equilibrium at a temperature of 1 K.

expansion of the phonon level density in the calculation of the canonical partition function). The result is

$$c \approx \sqrt{2\pi T^2 C_{ph}} A E^{-5/8}, \qquad (44)$$

where C_{ph} is again the phonon heat capacity. The leading order expressions for the phonon parameters $C_{ph}(T)$ and $E_{ph}(T)$ give, taking into account the different scaling of energies for phonons and ripplons, the total level density

$$\rho(E) = \rho_{rip}(E) 0.526 N^{1/6} \exp(0.047\,13 N^{-1/2} T^3$$
$$+ 0.013\,17 N^{1/3} T^2 + 0.1634 N^{1/6} T), \qquad (45)$$

with the equation given in ripplon energy units and $T = T(E)$ given by Eq. (15). The constant of 0.05 for the phonon level density preexponential, mentioned at the end of Sec. IV, was used here also.

This result is compared with the numerical convolution for $N = 10^3$ in Fig. 5. The numerical convolution was also calculated for $N = 10^4$ with a similar outcome.

One remark about Eqs. (43) and (45) is in order: These equations should only be used for calculations of microcanonical properties. For the calculation of canonical properties one should use the product partition function, $Z_{ripp,ph} = Z_{rip} Z_{ph}$. A naive application of Eq. (45) in a calculation of the partition function of the combined ripplon-phonon system will give a divergent result at all temperatures. The origin of this divergence is the breakdown at high excitation energies of the approximations leading to the equation.

VII. CONCLUSIONS

We have presented an analytical evaluation of the statistical density of state functions of the elementary excitations (surface ripplons and volume phonons) of isolated liquid-drop helium nanoclusters. These functions are expressed in terms of microcanonically conserved quantities: energy and

angular momentum. The obtained formulas accurately match numerically computed curves as the energy level densities vary over $\sim 150-300$ orders of magnitude.

Other interesting helium systems to which the results may be applicable include micron-sized superfluid fog[24] and multielectron bubbles in liquid helium. The latter are spherical voids inside bulk He, with a thin shell of electrons lining the inner wall (see, e.g., Refs. [25] and [26] and references therein). They can undergo small-amplitude shape oscillations, i.e., ripplons, whose frequency under zero external applied pressure has the form $\omega_\ell^2 \propto (\ell^2 - 1)(\ell - 2)$, which for large ℓ approaches the same form as the droplet ripplon dispersion [Eq. (1)]. This implies that the statistical mechanics of these bubbles should be similar to that of nanodroplets. One distinction is that the bubble is submerged into a bulk helium thermal bath; therefore, for them the canonical ensemble treatment is rigorously correct and not just a convenient approximation.

Finally, it should be pointed out that the results obtained in the present paper have a universal form and are expressed in terms of dimensionless scaled energies; therefore, they are generally applicable to the statistics of droplets of various substances besides helium.

APPENDIX

This appendix outlines details of the calculation performed between Eqs. (12) and (13) in the main text of the paper, and the inversion of the energy-temperature relation.

Evaluating the derivative in Eq. (12), we have, using L to denote the angular momentum,

$$\ln Z = -\int_2^\infty (2L+1)\ln(1 - e^{-\beta E_L}) dL$$

$$-\frac{7}{3}\ln(1 - e^{-\beta E_2}) + \frac{5}{12}\frac{\beta e^{-\beta E_2}\frac{dE_L}{dL}\Big|_{L=2}}{1 - e^{-\beta E_2}}, \quad (A1)$$

where $[dE_L/dL]_{L=2} = 7\sqrt{2}/4$ and $E_2 = \sqrt{8}$. In the high energy limit, the last two terms can be expanded to leading order in β, and they add up to $35/96 - (7/3)\ln(\beta 2\sqrt{2})$.

Next, the integral in Eq. (A1) needs to be evaluated, and this must be done beyond the leading order. The first step is a partial integration,

$$-\int_2^\infty (2L+1)\ln(1 - e^{-\beta E_L}) dL = -[(L^2 + L)\ln(1 - e^{-\beta E_L})]_2^\infty$$

$$+ \int_2^\infty (L^2 + L)\frac{\beta \frac{dE_L}{dL}}{e^{\beta E_L} - 1} dL. \qquad (A2)$$

The term in brackets is $\approx 6\ln(2\sqrt{2}\beta)$, and the second term is calculated by changing the integration variable to E_L, becoming $\int_{E_2}^{\infty}(L^2+L)\beta[e^{\beta E_L}-1]^{-1}dE_L$, with (L^2+L) considered a function of E_L. The relation between E_L^2 and L is a cubic equation and can be solved in closed form, but it is more instructive to use an iterative procedure [which below also will be applied to inverting the function $E(\beta)$] as follows. Equation (1) can be rewritten as $L=(E_L^2-L^2+2L)^{1/3}$ and expanded to give

$$L \approx E_L^{2/3}\left[1-\frac{1}{3}\frac{L^2}{E_L^2}+\frac{2}{3}\frac{L}{E_L^2}-\frac{1}{9}\left(\frac{L^2}{E_L^2}\right)^2\right]. \quad (A3)$$

This equation is used iteratively to eliminate all L's appearing on the right-hand side; after some algebra we get, to the same order in E_L,

$$L = E_L^{2/3} - \frac{1}{3} + \frac{7}{9}E_L^{-2/3}, \quad (A4)$$

The integral on the right-hand side of Eq. (A2) then becomes equal to

$$\int_{E_2}^{\infty}\left(E_L^{4/3}+\frac{1}{3}E_L^{2/3}+\frac{4}{3}\right)\frac{\beta}{e^{\beta E_L}-1}dE_L. \quad (A5)$$

The first two integrands are well behaved at zero and the corresponding integrals can be calculated as

$$\int_{E_2}^{\infty}E_L^{2n/3}\frac{\beta}{e^{\beta E_L}-1}dE_L = \int_{0}^{\infty}E_L^{2n/3}\frac{\beta}{e^{\beta E_L}-1}dE_L$$
$$-\int_{0}^{E_2}E_L^{2n/3}\frac{\beta}{e^{\beta E_L}-1}dE_L, \quad (A6)$$

with $n=1,2$. The second of these can be approximated by expanding the exponential to leading order in βE_L and evaluates to $(3/2n)E_2^{2n/3}$. The integrals from zero to infinity, in turn, are equal to (setting $x=\beta E_L$)

$$\beta^{-2n/3}\int_{0}^{\infty}x^{2n/3}\frac{1}{e^x-1}dx = \beta^{-2n/3}c_n, \quad (A7)$$

where the numerical constants can be expressed as

$$c_n = \int_{0}^{\infty}x^{2n/3}\sum_{j=1}^{\infty}e^{-jx}dx = \sum_{j=1}^{\infty}j^{-2n/3-1}\int_{0}^{\infty}x^{2n/3}e^{-x}dx, \quad (A8)$$

which is just a product of a sum and an integral (gamma and zeta functions). The values are $c_1=1.917\,00,\dots$ and $c_2=1.684\,94,\dots$.

Now, the last term in integral (A5), with $x=\beta E_L$ and leaving out the factor $4/3$, is

$$\int_{\beta E_2}^{\infty}\frac{1}{e^x-1}dx = \int_{\beta E_2}^{\infty}\sum_{j=1}^{\infty}e^{-jx}dx = \sum_{j=1}^{\infty}\frac{e^{-j\beta E_2}}{j} = -\ln(1-e^{-\beta E_2})$$
$$\approx -\ln(\beta E_2) = -\ln(2\sqrt{2}\beta). \quad (A9)$$

Collecting all the parts of Eq. (A5) and combining them in Eq. (A2) with its previously evaluated first term, we find that therefore

$$-\int_{2}^{\infty}(2L+1)\ln(1-e^{-\beta E_L}) \approx c_2\beta^{-4/3}+\frac{c_1}{3}\beta^{-2/3}-4$$
$$+\frac{14}{3}\ln(2\sqrt{2}\beta). \quad (A10)$$

Finally, bringing together all the parts of the Euler-Maclaurin expansion in Eqs. (12) and (A1), and keeping only terms of consistent orders of magnitude give

$$\ln Z \approx c_2\beta^{-4/3}+\frac{c_1}{3}\beta^{-2/3}-\frac{349}{96}+\frac{7}{3}\ln(2\sqrt{2}\beta). \quad (A11)$$

This is Eq. (13). Equation (14) for $E(\beta)$ follows directly from it with the help of Eq. (10),

$$E = \frac{4}{3}c_2\beta^{-7/3}+\frac{2}{9}c_1\beta^{-5/3}-\frac{10}{3}\beta^{-1}. \quad (A12)$$

To invert this equation, we again follow the iterative method and rewrite it as

$$\beta^{-1} = \left(\frac{3}{4c_2}\right)^{3/7}\left(E-\frac{2}{9}c_1\beta^{-5/3}+\frac{10}{3}\beta^{-1}\right)^{3/7}. \quad (A13)$$

Expanding this to the desired order and iterating, after a straightforward but tedious calculation, we arrive at

$$\beta^{-1} = \left(\frac{3}{4c_2}\right)^{3/7}E^{3/7}-\frac{2}{21}c_1\left(\frac{3}{4c_2}\right)^{8/7}E^{1/7}$$
$$+\left[\left(\frac{2}{21}c_1\right)^2\left(\frac{3}{4c_2}\right)^{13/7}\frac{5}{3}+\frac{10}{7}\left(\frac{3}{4c_2}\right)^{6/7}\right.$$
$$\left.-\frac{8}{49\times27}c_1^2\left(\frac{3}{4c_2}\right)^{13/7}\right]E^{-1/7}. \quad (A14)$$

This is Eq. (15).

*FAX: +46 (0)31 772 3496. klavs@physics.gu.se

[1] J. P. Toennies and A. F. Vilesov, Angew. Chem., Int. Ed. **43**, 2622 (2004).

[2] F. Stienkemeier and K. K. Lehmann, J. Phys. B **39**, R127 (2006).

[3] R. Guardiola, O. Kornilov, J. Navarro, and J. P. Toennies, J. Chem. Phys. **124**, 084307 (2006).

[4] The possibility of corrections to the liquid drop model excitation spectra, of vortex excitations in doped droplets, and of other finite-size effects have attracted interest in the literature, but no definitive results are available yet (see the review in Ref. 2).

[5] A. Tamura, Phys. Rev. B **53**, 14475 (1996).

[6] D. M. Brink and S. Stringari, Z. Phys. D: At., Mol. Clusters **15**, 257 (1990).

[7] K. K. Lehmann, J. Chem. Phys. **119**, 3336 (2003).

[8] K. K. Lehmann, J. Chem. Phys. **120**, 513 (2003).

[9] K. K. Lehmann and A. M. Dokter, Phys. Rev. Lett. **92**, 173401 (2004).

[10] L. D. Landau and E. M. Lifshitz, *Fluid Mechanics*, 2nd ed. (Butterworth-Heinemann, Oxford, 1987), Sec. 62.

[11] H. A. Bethe, Rev. Mod. Phys. **9**, 69 (1937).

[12] T. Ericson, Adv. Phys. **9**, 425 (1960).

[13] J. U. Andersen, E. Bonderup, and K. Hansen, J. Chem. Phys. **114**, 6518 (2001).

[14] *Handbook of Mathematical Functions*, edited by M. Abramowitz and I. A. Stegun (Dover, New York, 1972).

[15] T. Beyer and D. F. Swinehart, Commun. ACM **16**, 379 (1973).

[16] To resolve the numerical comparison, we employed two more digits on the leading order term in the exponential than written out in the text.

[17] C. Kittel, *Introduction to Solid State Physics*, 7th ed. (Wiley, New York, 1996).

[18] H. P. Baltes and E. R. Hilf, *Spectra of Finite Systems* (Bibliographisches Institut, Mannheim, 1976).

[19] H. P. Baltes and E. R. Hilf, Comput. Phys. Commun. **4**, 208 (1972).

[20] M. Brack and R. K. Bhaduri, *Semiclassical Physics* (Addison-Wesley, New York, 1997).

[21] H. P. Baltes and E. R. Hilf, Solid State Commun. **12**, 369 (1973).

[22] A. D. B. Woods and R. A. Cowley, Rep. Prog. Phys. **36**, 1135 (1973).

[23] M. W. Reynolds, I. D. Setija, and G. V. Shlyapnikov, Phys. Rev. B **46**, 575 (1992).

[24] H. Kim, K. Seo, B. Tabbert, and G. A. Williams, Europhys. Lett. **58**, 395 (2002).

[25] M. M. Salomaa and G. A. Williams, Phys. Rev. Lett. **47**, 1730 (1981).

[26] J. Tempere, I. F. Silvera, and J. T. Devreese, Phys. Rev. Lett. **87**, 275301 (2001).